

Article

Photo-Oxidation of Various Organic Compounds, Including Pollutants, by Europium (III) in Fuel Cell Systems

Felix Blind * and Stefan Fränze

International School Zittau (IHI), TUD University of Technology Dresden, Markt 23, D-02763 Zittau, Germany; stefan.fraenzle@tu-dresden.de

* Correspondence: felix.blind@mailbox.tu-dresden.de or felix.blind@gmx.de

Abstract: The ongoing anthropogenic climate crisis necessitates a reassessment of numerous technical domains, including the energy sector. An alternative to conventional fuel cells is provided by photo fuel cells, which possess at least one photoactive electrode (e.g., TiO₂). However, it should be noted that such fuel cells are often constrained in terms of the range of potential fuels that can be utilized. Considering prior research on the distinctive photochemistry of europium, it was hypothesized hypothesis that a photocell based on the photo-oxidation of diverse organic compounds by trivalent europium might be theoretically feasible. As demonstrated in multiple experiments, it is feasible to construct and operate a fuel cell utilizing these diverse, straightforward substrates. In this context, peak powers of up to 14 μ W have already been observed with the fuel cell described. It is noteworthy that an average electrical power of up to 6.28 μ W was observed over a period of 168 h (7 days). Furthermore, it was demonstrated that simple alcohols (ethanol) could be completely oxidized with trivalent europium under suitable conditions. From various studies with different ethanol concentrations, it could be seen that a certain amount of water was needed to break down simple alcohols and organic compounds in general.

Keywords: photo fuel cell; europium; photochemistry; fuel cell



Citation: Blind, F.; Fränze, S.

Photo-Oxidation of Various Organic Compounds, Including Pollutants, by Europium (III) in Fuel Cell Systems.

ChemEngineering **2024**, *8*, 121.

<https://doi.org/10.3390/chemengineering8060121>

<https://doi.org/10.3390/chemengineering8060121>

Academic Editor: Iuliana Deleanu

Received: 30 September 2024

Revised: 21 November 2024

Accepted: 25 November 2024

Published: 1 December 2024



Copyright: © 2024 by the authors. Licensee MDPI, Basel, Switzerland. This article is an open access article distributed under the terms and conditions of the Creative Commons Attribution (CC BY) license (<https://creativecommons.org/licenses/by/4.0/>).

1. Introduction

One of the causes of the current climate crisis is anthropogenic greenhouse gas emissions. These are directly linked to the burning of fossil fuels (coal, gas and oil), which has increased steadily since the industrial revolution. It is therefore essential to significantly reduce anthropogenic greenhouse gas emissions in the coming years to levels that existed before the start of the industrial revolution. This can only be achieved through a “new” revolution in the energy sector toward green, environmentally friendly alternatives. These include solar, wind and hydroelectric power. However, these have the major problem of not being available everywhere and, in the case of wind and hydroelectric power. Solar systems are much more flexible, but they are also tied to a specific location (orientation to the sun). In general, production and consumption sites are often far apart. In Germany, for example, the coastal regions in the north are particularly suitable for wind power generation, while the majority of consumers (industry) are located inland or even in the south. As a result, electricity must often be transported over long distances, which is usually possible using a normal electricity grid. The transportation sector (e-mobility) is more of a problem. There are generally two different approaches to e-mobility. The first is to run an electric car on batteries, but this currently has the major disadvantage that such vehicles have a comparatively short range, which tends to make them impractical in certain areas (including freight transport). In addition, the batteries used often bind many rare raw materials, and at the end of their useful life, they must often be disposed of in a complex and costly manner. As a result, the actual disposal often takes place in developing countries, where improper working practices can lead to environmental pollution. An alternative is

the fuel cell, which can be used in any size, both on-site and in vehicles. Although fuel cells also bind a certain amount of rare raw materials (e.g., platinum group metals), they have a much longer lifetime than conventional batteries. Conventional fuel cells can be broadly categorized as the following:

- Proton-exchange membrane fuel cells (PEMFCs);
 - Low-temperature-PEMFC;
 - High-temperature-PEMFC;
- Direct methanol fuel cell (DMFC);
- Phosphoric acid fuel cell (PAFC);
- Molten carbonate fuel cell (MCFC);
- Solid oxide fuel cell (SOFC);
- Alkaline fuel cell (AFC).

What they all have in common is that they mostly use hydrogen (H_2) and oxygen (O_2) as fuels. Especially in the mobility sector, this hydrogen must be stored and transported safely, sometimes over long distances. However, storage in individual vehicles is often problematic. As a result, fuel cell vehicles are still relatively rare. Direct methanol fuel cells (DMFCs) can be used; methanol ($MeOH$) is much easier and safer to transport and store than H_2 . Another major advantage of such fuel cells is that they operate at comparatively mild temperatures in the range of $60\text{ }^\circ\text{C}$ to $120\text{ }^\circ\text{C}$. However, the problem with such fuel cells is that $MeOH$ can diffuse through various membranes and reach the cathode side of a fuel cell. As a result, $MeOH$ is oxidized at the cathode, causing the electrical potential and efficiency to drop [1].

Another promising type of fuel cell has been described in the literature for about two decades. These are photocatalytic fuel cells, which have at least one photocatalytically active electrode (TiO_2/FTO , $BiVO_4/FTO$ or $W-BiVO_4/V_2O_5$) [2–5]. Fuel oxidation typically occurs at this electrode (photoanode), while the reduction of oxygen or other suitable electron acceptors occurs at the cathode [4,6], as shown in Figure 1.

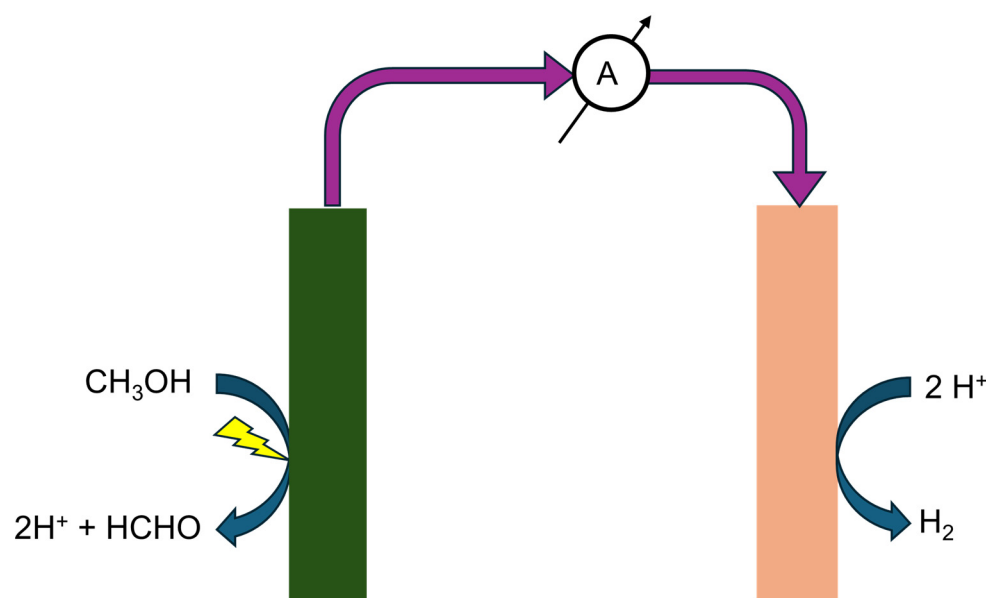
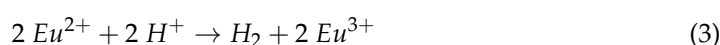
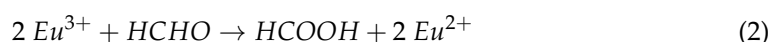
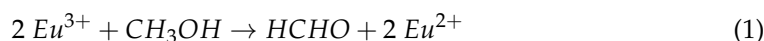


Figure 1. Schematic representation of a single chamber photo fuel cell. The green component represents the photoanode, which is composed of a photoactive material (e.g., TiO_2) for the oxidation of suitable fuels (in this case, methanol). The orange component depicts the cathode, which is responsible for the reduction of H^+ to H_2 .

As shown in Figure 1, such fuel cells can also be designed as single chamber systems [4]. This means that, at least in theory, the use of expensive membranes (e.g., Nafion[®]) and electrode materials (platin group metals) can be dispensed. While the first photocatalytic

fuel cells often used hydrogen peroxide (H₂O₂) as a fuel [4,7,8], a variety of organic compounds are used today. These include simple alcohols such as methanol, ethanol or propanol [9], as well as more complex compounds such as azo dyes [10].

The fuel cell described in this paper is a modification of the previously mentioned fuel cells. The main difference is that it was not the electrodes that were photocatalytically active, but a photocatalyst added to the reaction medium, in this case, europium. It has been known for about 50 years that simple organic compounds (methanol, formic acid) can be photocatalytically oxidized with trivalent europium. As shown in the following simplified reaction diagram, this is a redox reaction, in which Eu²⁺ is produced Or, respectively, consumed (Equations (1)–(3)) [11].



As already described in the literature, this can be used to photocatalytically reduce various organic compounds or can be oxidized at suitable electrodes to produce Eu³⁺ and start the cycle again. The authors also showed that these reactions could take place with diffuse sunlight. Europium is particularly well suited for this purpose due to its outstanding and unique properties, i.e., being widely used today as a dopant in semiconductors and for its fluorescent properties in the lighting industry. What is less well known is that trivalent europium in particular is an exceptionally good oxidizing/dehydrogenating agent in its low excited state, produced by irradiation at $\lambda \approx 394$ nm. Contrary to widespread belief, europium can be used to break down organic compounds that are much more complex than methanol or formic acid. We showed in [12] that this capability does include various environmental pollutants such as those present in wastewater, like chlorobenzene. In this context, we already showed that the spectrum of organic compounds that can be converted with trivalent europium is broader than previously thought [13].

This finding, that Eu(III) oxidizes a wide range of organic substances, led us to the hypothesis that it might be possible to design a photo fuel cell based on the photochemistry of europium. This proof-of-concept study describes the performance characteristics for different simple organic substances like ethanol, acetic acid and glucose fur such as photo fuel cell in an early experimental stage.

2. Materials and Methods

2.1. Description of the Self-Constructed Photo Fuel Cell

Based on preliminary “proof-of-principle tests”, which were analogous in structure to the original design of the gas battery described by Schönbein [14,15], the test fuel cell depicted in Figure 2 was developed in several stages. As can be observed, the fundamental structure comprises commercially available PVC pipes (1 Zoll), which are also utilized in the sanitary sector. The authors selected PVC pipes at this juncture due to their chemical and pressure resistance. Additionally, the systems can be expanded with relative ease, as evidenced by their screw connections. The selected design also permits the insertion of various measuring devices (pH meter, thermometer) into the fuel cells without the necessity for significant modifications.

In all the experiments described in this study, tantalum electrodes of varying shapes and an average surface area of approximately 8 cm² were used. The photoreaction chamber was illuminated by a standard flexible color-changing LED strip set to pink. The emission spectrum for this setting showed a wide peak under 400 nm as well as three peaks in the ranges of 455–465 nm, 485 nm and 670–680 nm.

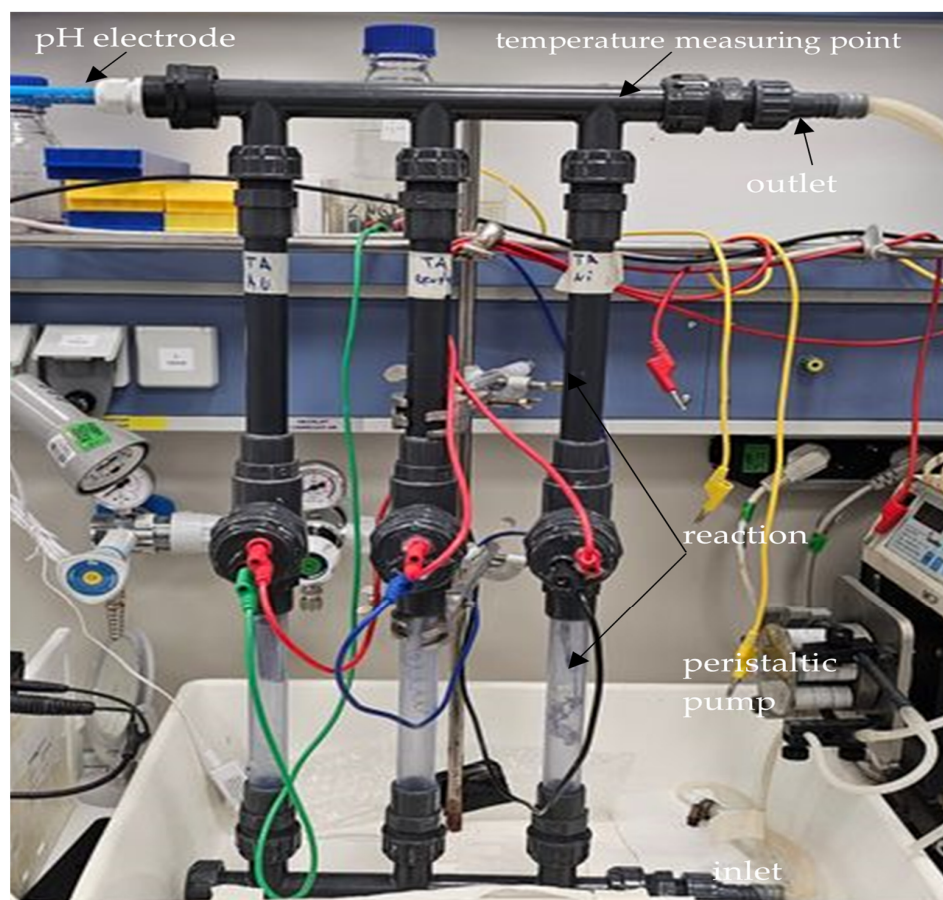


Figure 2. The self-designed fuel cell, which features a total of three reaction chambers. This configuration enables the simultaneous examination of up to three distinct electrode pairs, encompassing variations in material composition or shape.

2.2. Analysis of Various Possible Fuels for the Planned Fuel Cell Application

An overview of the simple organic compounds investigated and the exact compositions of the respective reaction batches are given in Table 1. In order to analyze their suitability as fuels in the fuel cell investigated here, they were first dissolved in demineralized water and transferred to a 2 L reaction vessel. The reaction solution was then pumped through the fuel cell (flow rate: 477 mL/min) for about 15 min. Subsequently, 2 mM Eu(III)-triflate (Sigma-Aldrich, 52093-25-1) and 2 mM of tetrabutylammonium tetrafluoroborate (TBA-TFB), listed in Table 1, were added and the reaction mixture was analyzed for at least 30 min. The supplemental light was then turned on and the measurement continued for up to 168 h. The operating parameters under study (pH, current and temperature) were checked periodically, and the reaction was terminated when either the measured current dropped to the initial level or the maximum planned reaction time was reached.

Table 1. A comprehensive overview of the compositions of the various reaction mixtures.

Substrate	Concentration	Conductive Salt	Eu(III)-Triflate ⁵	Total Volume
Ethanol ¹	10.0% (v/v)			
Ouzo (Ethanol)	70.0% (v/v)			
Ethanol ¹	99.5% (v/v)	TBA-TFB ⁴	2 mM	2 L
Acetic acid ²	25.0% (v/v)			
Glucose ³	20 mM			

¹ (VWR-Chemicals, Darmstadt, Germany, 64-17-5); ² Commercial vinegar essence; ³ (Fluka, Buchs, Switzerland, 50-99-7); ⁴ Tetrabutylammonium tetrafluoroborate (Fluka, Buchs, Switzerland, 429-92-5); ⁵ (Sigma-Aldrich, Taufkirchen, Germany, 52093-25-1).

2.3. Product Extraction with Toluene

For this purpose, 20 mL of toluene (Sigma-Aldrich; 108-88-3) was added to an aliquot of 100 mL of the reaction mixture and stirred for at least 24 h at 300 rpm in a sealed reaction vessel. After phase separation, the organic phase was removed and stored in a suitable reaction vessel in the dark at 6 °C until the organic compounds contained were analyzed using the GC-MS method.

2.4. Qualitative Analysis of Intermediate and End Products Occurring in the Described Fuel Cell Application

Since the reactions catalyzed by europium are mostly redox reactions with one or more radical intermediates, it was essential to evaluate the quality of the resulting products, although with respect to possible contaminants (special attention was paid to possible environmental pollutants and substances harmful to the processes taking place in the fuel cell). For the GC-MS method, described before by Blind, the samples were first analyzed natively [13]. However, since most of the more complex organic compounds were comparatively poorly volatile, they could not be easily analyzed by the GC-MS method described. The prepared samples were silylated and then reanalyzed. For this purpose, 10 µL of silylating agent (N-t-butyl-N-trimethylsilyl-trifluoroacetamide (Supelco)) was added to an aliquot of 1 mL of the sample and the reaction mixtures were stored at 60 °C for 20 min. The samples were then reanalyzed as soon as possible to avoid the outgassing of the silylated products. Note that no qualitative product analysis was performed due to the continuous process control.

2.5. Theoretical Estimation of the Eu (III)/Eu (II) Ratio

On the assumption that the determined potential was the result of the oxidation of Eu(II) ions at the anode, it was possible to estimate the approximate ratio of Eu(III)/Eu(II) using the Nernst equation (Equation (A1)). In this study, the standard electrode potential for the redox couple Eu(III)/Eu(II) was derived from the literature value of -0.350 V (vs. NHE, valid for pH = 0 . . . 7.5) in water [16–18].

3. Results

3.1. Overview of Selected Performance Parameters of the Fuel Cell as a Function of the Substrates Examined

Figure 3 depicts the electrical power of the fuel cell described in this investigation for the substrates under consideration. As illustrated, peak electrical outputs of up to 276.88 nW (glucose) were observed for all substrates, except for acetic acid. It is important to note, however, that the mean electrical power for the substrates examined differed significantly in some cases, with values ranging from approximately 6 nW to 210 nW. The differences between the samples with 10.00% and 99.95% ethanol concentrations were particularly noteworthy. The peak power observed for acetic acid was approximately 14 µW, while the average electrical power was approximately 6.28 µW.

Based on the process parameters (current and voltage) presented in Table A1, the calculated $\text{Eu}^{3+}/\text{Eu}^{2+}$ ratios are presented in Table 2. As illustrated, these spanned a range from 9.784×10^6 (glucose) to 1.343×10^8 (acetic acid). As evidenced in Table 2, these ratios suggest that a significant portion of the europium utilized was present in the reaction mixture in a trivalent state.

Table 2. Overview of the determined ratios of $\text{Eu}^{3+}/\text{Eu}^{2+}$ and the resulting concentrations of Eu^{3+} and Eu^{2+} .

Substrate	Ratio $\text{Eu}^{3+}/\text{Eu}^{2+}$	$c(\text{Eu}^{2+})$ [mM]	$c(\text{Eu}^{3+})$ [mM]
EtOH 10.00%	1.075×10^7	2.326×10^{-7}	
EtOH 99.95%	1.074×10^7	2.326×10^{-7}	Ca. 2.5
Ouzo	9.784×10^6	2.556×10^{-7}	

Table 2. Cont.

Substrate	Ratio $\text{Eu}^{3+}/\text{Eu}^{2+}$	$c(\text{Eu}^{2+})$ [mM]	$c(\text{Eu}^{3+})$ [mM]
Acetic acid 25%	1.343×10^8	1.861×10^{-6}	Ca. 2.5
Glucose	1.100×10^7	2.273×10^{-7}	

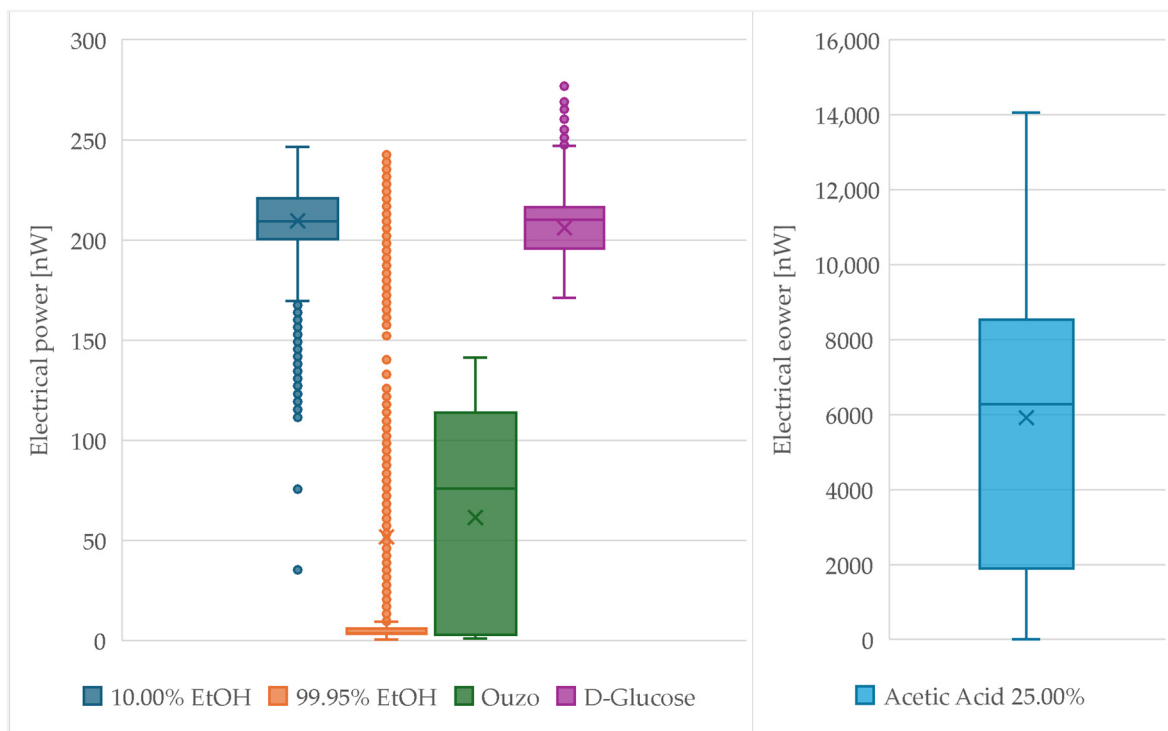


Figure 3. Overview of the electrical power of the power parameters described in this work for the substrates/fuels examined.

3.2. Results of the Product Analysis for the Conversion of the Examined Substrates Using Eu^{3+}

3.2.1. Results of the Product Analysis for the Implementation of Ethanol

The analysis of the products of the conversion of ethanol with trivalent europium in the fuel cell described here revealed the formation of several additional products, in addition to the expected acetaldehyde and acetic acid. These were methanol and acetic acid. It is important to note, however, that as can be observed in Figure A1, the reaction mixture clearly turned greenish, which could indicate the presence of differently colored products or differently complexed metal ions. Furthermore, the reaction mixture exhibited a distinct banana-like odor, which suggests that the reaction generated additional volatile compounds (butyl or pentyl esters of acetic acid).

3.2.2. Results of the Product Analysis for the Implementation of Ouzo

As anticipated, the products resulting from the conversion of ouzo with trivalent europium in the fuel cell exhibited similarities. The analysis revealed the formation of methanol, acetaldehyde, acetic acid and 2-propanone. Furthermore, other products were identified as the following:

- Xylene;
- Methylbenzene;
- Ethylbenzene;
- 1,3-Cyclohexanedione enol;
- 1-Ethyl-5,2-cyclohexene-1-one;
- Bicyclo(2,2,2)octane-2,6-dione;

- 1H- Xanthene-1,8-(2H)dione-3,4,5,6,7,9-hexahydrate.

As with the conversion of “pure” ethanol, the reaction mixture in the conversion of ouzo exhibited a distinct green coloration and an odor reminiscent of a banana upon cessation of the experiment. This suggests the presence of previously undetectable compounds. It is also noteworthy that the aniseed odor characteristic of ouzo became more pronounced as the test progressed, eventually becoming undetectable at the conclusion of the experiment. This observation suggests that the anisaldehydes in question could be converted in the fuel cell with trivalent europium, either directly or indirectly, through various reactions that have not yet been fully elucidated.

3.2.3. Results of the Product Analysis for the Implementation of Acetic Acid

The product analysis of the reaction of acetic acid showed that in addition to low-molecular-weight organic compounds, higher-molecular-weight compounds were also formed. In addition to methanol, the low-molecular-weight organic compounds included 3-butene-2-one, 1-pentene-3-one, 2-pentene-4-one, 2-ketoglutaric acid and hexanedioic acid. Higher-molecular-weight compounds included dodecane, tetradecan-5-one, hexadecane and oleic acid. Similar to the reactions of ethanol and ouzo, a greenish to yellowish discoloration of the reaction mixture was also observed in the reaction of acetic acid with trivalent europium. Although the reaction mixtures for the conversion of acetic acid also exhibited a fruity odor at the end of the reaction, it could not be identified due to a strong vinegar note. This clearly indicated that acetic acid must have still been present in the solution after the reaction was stopped.

3.2.4. Results of the Product Analysis for the Implementation of Glucose

Despite the application of silylation to any products present, the product analysis for the conversion of glucose using the GC-MS method described here remained inconclusive. This indicates, among other things, that glucose could be completely degraded into CO₂ and H₂O with trivalent europium. The loss of approximately 100 mL of liquid and the clear yellow coloration of the reaction mixture suggest that several side reactions occurred during the conversion of glucose in the fuel cell described here. The resulting products are likely to have been high-molecular-weight compounds that could not be detected with the chosen GC/MS method. Furthermore, the pleasant fruity odor indicated that a range of esters may have also been produced during the reaction.

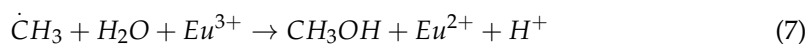
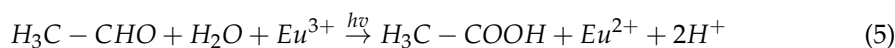
4. Discussion

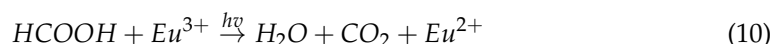
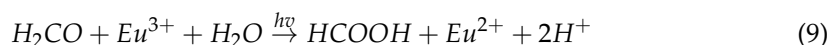
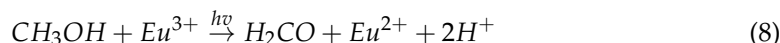
4.1. Discussion of the Reaction of the These Substances with Eu³⁺ in the Fuel Cell

4.1.1. Discussion of the Reaction of Ethanol and Acetic Acid with Eu³⁺ in the Fuel Cell

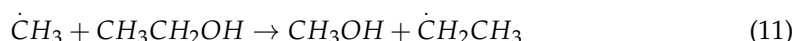
As previously stated, the mean power of the experiments conducted with ethanol concentrations of 10.00% and 99.95% exhibited a notable discrepancy, contrary to our initial expectations. Given that the same substrate (ethanol) was employed in both cases, this outcome is incongruous with our expectations. Consequently, a detailed discussion of this result is provided below. The complete oxidation of ethanol with trivalent europium has been described in the literature as a reaction mechanism comprising the following steps, which are shown in Equations (4)–(10) [11,19–23].

As can be seen in Equation (7), the intermediate products require the presence of water to undergo their subsequent transformations and complete the reaction [11].





The observed discrepancies in performance between the experiments with an ethanol concentration of 10.00% and 99.95%, respectively, can most likely be attributed to the presence of water. This indicates that the primary products of the breakdown of pure ethanol should be acetaldehyde and acetic acid. However, the identification of methanol and formic acid as products suggests that methanol may have also been formed because of a reaction between the methyl radical and ethanol (cf. Equation (11)). The significantly lower power yield indicates that this reaction is less favorable thermodynamically than the reaction with water (cf. Equation (7)).

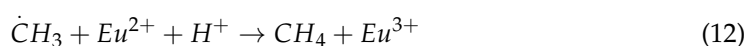


The discoloration of the ethanol-containing reaction mixtures and the fruity odor observed at the conclusion of the reaction may have been attributed to side reactions of the radicals, which produce esters and occur in accordance with the proposed Equations (7) and (11) (in organic solvents, Eu(III)* does transfer ester groups to alkenes, imines, etc.). At this juncture, it is not possible to discount the possibility of further radical formation, which could explain the synthesis of a range of complex organic compounds, some of which may not have been detectable using the aforementioned GC-MS methodology. Concurrently, the formation of various esters, including ethyl acetate, may have been a potential consequence of these reactions. It is also possible that esterification reactions may have occurred. It should be noted, however, that most of the technical esterification was conducted at considerably higher temperatures and under excess pressures with the use of suitable catalysts [24,25]. The formation of esters by a Tishchenko reaction catalyzed by REE complexes in organic solvents was previously described, yet only occurred when using *N,N*-bis-trisilylamides of, e.g., Nd and at rather high temperatures. The finding that the fruity smell eventually disappeared agrees with the capacity of photoexcited Eu(III) not only to abstract H atoms from C- or N-atoms or change the size of rings but also to transfer ester groups inside one and among different or identical molecules. This renders the occurrence of such a reaction highly improbable, yet it cannot be entirely dismissed. The decomposition products of the acetic acid reaction could be elucidated at this juncture with the aid of Equations (6)–(11) (methanol and formic acid) and the advent of assorted radical reactions (3-butene-2-one, 1-pentene-3-one, 2-pentene-4-one, 2-ketoglutaric acid and adipic acid). For purposes of clarity, the authors will refrain from delving into the intricacies of the radical reactions that may have ensued at this stage.

4.1.2. Discussion of the Reaction of Ouzo with Eu^{3+} in the Fuel Cell

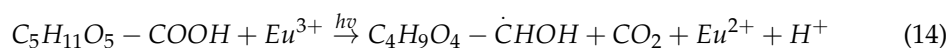
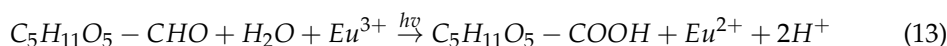
It is widely acknowledged that ouzo is an aniseed-flavored liquor originating from Greece. Typically, it has an ethanol content of approximately 40% [26]. Thus, the authors anticipated an electrical output comparable to that observed in the experiment with 10.00% ethanol content. Nevertheless, the results demonstrated that this was markedly lower (ouzo: 75.84 nW; EtOH 10.00%: 209.25 nW). However, this cannot be attributed to the lack of water (see Equation (7)), which primarily indicates that additional limiting factors must have been present (in molar fraction terms, the main component of ouzo still was water). Some additional compounds obviously have a detrimental impact on the photoreaction of trivalent europium or exert a direct influence on electrode reactions. In general, ouzo, like other anise-based liquors, contains not only water and ethanol but also a variety of additional compounds, including various fusel alcohols (e.g., 2-propanol, 3-pentanol, 1-hexanol), aldehydes (e.g., acetaldehyde), various esters and other volatile organic substances (4-propenyl anisole, also known as anethole) [26]. In this context, the literature

describes up to 60 different ingredients for ouzo [26]. In light of Blind's demonstration that a vast array of organic compounds can be photochemically oxidized with trivalent europium, it can be assumed that a number of side reactions must have occurred during the reaction of ouzo [13]. This would also explain the observed broad product spectrum. However, this does not initially explain why the electrical power was significantly lower when ouzo was used. It is assumed that the bivalent europium produced was not oxidized at the anode, but rather reduced into trivalent europium through the reduction of various organic compounds. The observed low power yield was anticipated. This lends support to the earlier assumption. A review of the literature revealed that simple organic compounds can be photochemically reduced by bivalent europium (see Equation (12)) [11]. Thus far, however, such reactions have only been described in the literature for simple organic compounds [11,27,28]. Nevertheless, this indicates that under suitable conditions, the formed bivalent europium can undergo photochemical reactions, resulting in a decrease in the oxidized portion at the anode and a significant reduction in the observed power output of the fuel cell. It can be postulated that a combination of factors was responsible for this decrease in power. Therefore, further examination of the photochemistry of divalent europium was warranted.



4.1.3. Discussion of the Reaction of Glucose with Eu^{3+} in the Fuel Cell

Given the inconclusive nature of the product analysis for the implementation of glucose with Eu^{3+} , it was not possible to make any qualified statements regarding possible degradation pathways at this stage. However, the conspicuous discoloration and the distinctly fruity odor, in combination with the determined mean electrical power of about 210 nW, indicated that glucose could indeed be oxidized with the help of trivalent europium. As illustrated in Equation (12), the decomposition of glucose, akin to that of numerous other reducing sugars, occurs via gluconic acid as the initial intermediate. A closer examination of the degradation pathway for ethanol revealed that it also proceeds via the corresponding carboxylic acid. At this juncture, the authors hypothesize that a reaction analogous to that depicted in Equation (7) may have ensued (cf. Equations (13) and (14)). Given the disparate points of attack for oxidation with trivalent europium, it is plausible that disparate radicals could have been formed. Nevertheless, the reaction of these radicals would likely have resulted in the formation of relatively high-molecular, more complex organic compounds. This would also explain the negative result of the product analysis, as many of these high-molecular organic compounds are not readily detectable by gas chromatography. Concurrently, the presence of a fruity odor suggests that glucose was undergoing partial further breakdown, which could potentially result in the formation of various volatile organic compounds, including esters. Considering these findings, further research is required to investigate the reaction of glucose with trivalent europium.



4.2. Comparison of the Electrical Power with That Already Described for Photo Fuel Cells

As shown, the average electrical power of the photo fuel cells described in this work ranged from 6 nW to 14 μ W. This was about 10–1000 times lower than the electrical power of the photo fuel cells already described in Table 3. This finding initially appeared to contradict the photo fuel cell based on trivalent europium as described in this work. Nevertheless, the data presented here, which were not previously published, indicated that the performance of the described fuel cell could be enhanced with relative ease. These possibilities will be discussed in brief below. Previously unpublished data indicated that the performance could be markedly enhanced by merely elevating the europium concentration. This can be

attributed to the fact that higher turnover rates can be achieved, which, in turn, increases the power. Another method for enhancing the power output, as previously demonstrated by Blind, is to incorporate chitin into the anode region [12]. However, due to technical limitations, this was not feasible with the fuel cell depicted in Figure 2, as chitin tends to expand in aqueous environments, potentially leading to fuel cell obstruction. The addition of chitin resulted in an increase in the electrical power of an earlier version of the fuel cell described here, reaching 56.34 μW for the substrate ethanol. This corresponds to an increase in power by a factor of approximately 262, placing the electrical power of the fuel cell described within the range of existing photo fuel cells. Furthermore, a photo fuel cell based on europium has the advantage of being able to operate with significantly more organic fuels than previous photo fuel cells. However, further investigation is required to ascertain the performance of the fuel cell described in this work.

Table 3. Overview of the electrical outputs of various photo fuel cells widely described in the literature.

Material Photoanode	Fuel	Electrical Power	Reference
0.53% Ag-BiOI/ITO	Bisphenol A	4.40 μW	[29]
W:BiVO ₄	Glucose	82 μW	[30]
TiO ₂	Glucose	36 μW	[31]
TiO ₂	Wastewater (brewery)	88.8 μW	[12]
BiVO ₄	Hydrogen peroxide	0.13 mW	[3]
BiVO ₄ /TiO ₂	Glucose	0.12 mW	[32]
BiVO ₄ /AgBr	Glucose	40 μW	[33]
BiVO ₄ /NiFe-LDH	Glucose	70 μW	[34]

Another possibility for increasing the power of the described fuel cell was to combine it with a conventional photo fuel cell and thus exploit the advantages of both systems. A schematic representation of such a combined fuel cell is shown in Figure A2.

4.3. Discussion of the Observed Power Fluctuations for the Tested Substrates

The performance of a fuel cell depends on the chemical reactions occurring at its electrodes. In general, an increase in the number of reactions occurring will result in an improvement in its performance. It should be noted that this also applies to the fuel cell described in this text. As previously stated, the oxidation of Eu(II) ions to Eu(III) ions at the anode resulted in the transfer of an electron to the anode. Concurrently, suitable electron acceptors were reduced at the cathode. The performance of the fuel cell described here is therefore contingent upon the quantity of Eu(II) ions that can be oxidized at the anode. As previously stated, several photocatalyzed side reactions occur in which Eu(II) ions are directly involved [11]. However, this results in competition between the unknown side reactions and the desired anode reaction, reducing the effective concentration of Eu(II) ions. Fluctuations in the concentration of Eu(II) ions consequently lead to variable electrode processes, which negatively impact the performance of the fuel cell.

5. Conclusions

In conclusion, it was possible to design a photo fuel cell based on the photochemistry of trivalent europium. It is important to note, however, that the performance of such a fuel cell is still subject to the following limiting factors:

1. The quantity of Eu(II) ions undergoing oxidation at the anode (donating electrons to it) rather than causing secondary photo- or thermochemical reactions in solution;
2. A variety of photoreactions involving Eu(II) ions and different organic compounds;
3. Previously unidentified side reactions potentially occurring at the anode or cathode.

The influencing factors resulted in a notable decline in the performance of the photo fuel cell in question, when compared to the performance of previously described photo fuel cells. As the power output is directly proportional to the concentration of Eu(II) ions,

an increase in power can be achieved by increasing the Eu concentration. Nevertheless, as this also facilitates the promotion of reactions, further research is required at this juncture to ascertain the most efficacious means of preventing such reactions. One potential avenue for further investigation could be the combination of the fuel cell described in this work with a conventional photo fuel cell, with the aim of specifically breaking down the organic substances that can be reduced by Eu(II). This would also have the side effect of significantly increasing the fuel cell's output. Another possibility for increasing the output of the described fuel cell system could be to utilize the hydrogen produced at the cathode in a conventional fuel cell.

In general, it can be stated that the photo fuel cell described here is a promising system in itself, but further investigation is required.

Author Contributions: Data curation, F.B.; formal analysis, F.B.; writing of the manuscript, F.B.; supervision, S.F. All authors have read and agreed to the published version of the manuscript.

Funding: This research received no external funding.

Institutional Review Board Statement: Not applicable.

Data Availability Statement: Dataset available on request from the authors.

Acknowledgments: We would like to thank Martin Kluge for his help with the GC-MS analysis.

Conflicts of Interest: The authors declare no conflicts of interest.

Appendix A

$$E = E^0 + \frac{59 \text{ mV}}{z_e} \log \left(\frac{\alpha_{ox}}{\alpha_{Red}} \right) \quad (\text{A1})$$

Appendix B

Table A1. Overview of the minimum, maximum and average currents and voltages determined for the substrates tested.

Substrate	Current			Voltage		
	Min. [μA]	Max. [μA]	$\bar{\text{O}}$ [μA]	Min. [mV]	Max. [mV]	$\bar{\text{O}}$ [mV]
EtOH 10.00%	10.86	28.66	26.40	3.26	8.60	7.92
EtOH 99.95%	1.22	28.64	5.62	0.37	8.59	2.59
Ouzo	1.17	21.71	12.01	6.35	6.51	3.60
Acetic acid 25%	6.03	216.47	125.91	1.81	64.94	37.77
Glucose	23.88	30.38	26.15	7.16	9.11	7.86

Appendix C



Figure A1. Greenish discoloration of the reaction mixture EtOH 10.00% after the reaction. The greenish discoloration shown appeared between 24 and 48 h after the photoreaction with Eu(III) was started and became more intense over time.

Appendix D

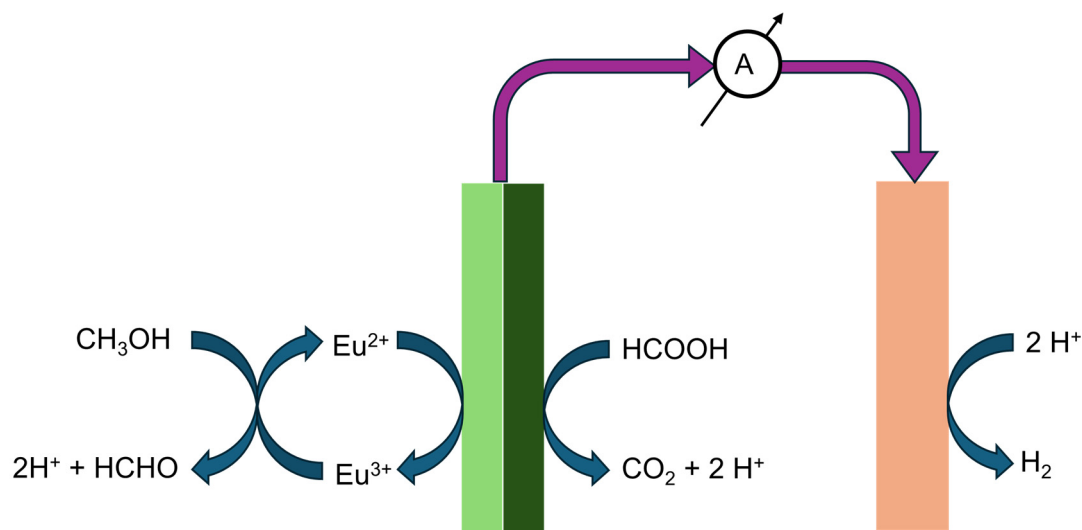


Figure A2. Schematic representation of a combination of a conventional photo fuel cell with the europium-based photo fuel cell described in this work.

References

1. Kurzweil, P. *Brennstoffzellentechnik: Grundlagen, Komponenten, Systeme, Anwendungen*; Springer Vieweg: Wiesbaden, Germany, 2013.
2. Sena, I.C.; Sales, D.d.O.; Andrade, T.S.; Rodriguez, M.; Da Silva, A.C.; Nogueira, F.G.E.; Rodrigues, J.L.; de Mesquita, J.P.; Pereira, M.C. Photoassisted chemical energy conversion into electricity using a sulfite-iron photocatalytic fuel cell. *J. Electroanal. Chem.* **2021**, *881*, 114940. [[CrossRef](#)]
3. Onishi, T.; Fujishima, M.; Tada, H. Solar-Driven One-Compartment Hydrogen Peroxide-Photofuel Cell Using Bismuth Vanadate Photoanode. *ACS Omega* **2018**, *3*, 12099–12105. [[CrossRef](#)] [[PubMed](#)]
4. Akita, A.; Masuda, T.; Fujiwara, K.; Fujishima, M.; Tada, H. One-Compartment Hydrogen Peroxide-Photofuel Cell Using TiO_2 Photoanode and Prussian Blue Cathode. *J. Electrochem. Soc.* **2018**, *165*, F300–F304. [[CrossRef](#)]
5. Kaneko, M.; Nemoto, J.; Ueno, H.; Gokan, N.; Ohnuki, K.; Horikawa, M.; Saito, R.; Shibata, T. Photoelectrochemical reaction of biomass and bio-related compounds with nanoporous TiO_2 film photoanode and O_2 -reducing cathode. *Electrochem. Commun.* **2006**, *8*, 336–340. [[CrossRef](#)]
6. Iyatani, K.; Horiuchi, Y.; Moriyasu, M.; Fukumoto, S.; Cho, S.-H.; Takeuchi, M.; Matsuoka, M.; Anpo, M. Development of separate-type Pt-free photofuel cells based on visible-light responsive TiO_2 photoanode. *J. Mater. Chem.* **2012**, *22*, 10460. [[CrossRef](#)]
7. Masuda, T.; Fujishima, M.; Tada, H. Photo-effect on the electromotive force in two-compartment hydrogen peroxide-photofuel cell. *Electrochem. Commun.* **2018**, *93*, 31–34. [[CrossRef](#)]
8. Zhang, B.; Wang, S.; Fan, W.; Ma, W.; Liang, Z.; Shi, J.; Liao, S.; Li, C. Photoassisted Oxygen Reduction Reaction in H_2 - O_2 Fuel Cells. *Angew. Chem.* **2016**, *128*, 14968–14971. [[CrossRef](#)]
9. Sfaelou, S.; Lianos, P. Photoactivated Fuel Cells (PhotoFuelCells). An alternative source of renewable energy with environmental benefits. *AIMS Mater. Sci.* **2016**, *3*, 270–288. [[CrossRef](#)]
10. Chen, Y.-A.; Yang, H.; Ouyang, D.; Liu, T.; Liu, D.; Zhao, X. Construction of electron transfer chains with methylene blue and ferric ions for direct conversion of lignocellulosic biomass to electricity in a wide pH range. *Appl. Catal. B Environ.* **2020**, *265*, 118578. [[CrossRef](#)]
11. Matsumoto, A.; Azuma, N. Photodecomposition of europium(III) acetate and formate in aqueous solutions. *J. Phys. Chem.* **1988**, *92*, 1830–1835. [[CrossRef](#)]
12. Lui, G.; Jiang, G.; Fowler, M.; Yu, A.; Chen, Z. A high performance wastewater-fed flow-photocatalytic fuel cell. *J. Power Sources* **2019**, *425*, 69–75. [[CrossRef](#)]
13. Blind, F. Orientierende Untersuchungen zur Platinmetall-freien Aktivierung von CH-Bindungen für Europium-basierte Brennstoffzellenanwendungen. Master's Thesis, TU Dresden, Dresden, Germany, June 2018.
14. Grove, W.R. *The Correlation of Physical Forces*; Longmans, Green: London, UK, 1874.
15. Schönbein, C.F. Neuen Beobachtungen über die Volta'sche Polarisierung fester und flüssiger Leiter. *Ann. Phys. Chem.* **1839**, *123*, 101. [[CrossRef](#)]
16. Morss, L.R. Thermochemical properties of yttrium, lanthanum, and the lanthanide elements and ions. *Chem. Rev.* **1976**, *76*, 827–841. [[CrossRef](#)]
17. Cokal, E.J. *Electroanalytical Chemistry of the Rare-Earths*; The University of Arizona: Tucson, AZ, USA, 1963.

18. Arman, M.Ö.; Geboes, B.; van Hecke, K.; Binnemans, K.; Cardinaels, T. Kinetics of electrochemical Eu³⁺ to Eu²⁺ reduction in aqueous media. *Electrochim. Acta* **2024**, *484*, 144055. [[CrossRef](#)]
19. Andrade, T.S.; Dracopoulos, V.; Keramidas, A.; Pereira, M.C.; Lianos, P. Charging a vanadium redox battery with a photo(catalytic) fuel cell. *Sol. Energy Mater. Sol. Cells* **2021**, *221*, 110889. [[CrossRef](#)]
20. Andrade, T.S.; Dracopoulos, V.; Pereira, M.C.; Lianos, P. Unmediated photoelectrochemical charging of a Zn-air battery: The realization of the photoelectrochemical battery. *J. Electroanal. Chem.* **2020**, *878*, 114709. [[CrossRef](#)]
21. Andrade, T.S.; Pereira, M.C.; Lianos, P. High voltage gain in photo-assisted charging of a metal-air battery. *J. Electroanal. Chem.* **2020**, *878*, 114559. [[CrossRef](#)]
22. Andrade, T.S.; Sá, B.A.C.; Sena, I.C.; Neto, A.R.S.; Nogueira, F.G.E.; Lianos, P.; Pereira, M.C. A photoassisted hydrogen peroxide fuel cell using dual photoelectrodes under tandem illumination for electricity generation. *J. Electroanal. Chem.* **2021**, *881*, 114948. [[CrossRef](#)]
23. Tennakone, K.; Ketipearachchi, U.S. The catalysis of hydrogen photogeneration from aqueous solutions of alcohols by the samarium(III) and europium(III) ions. *Chem. Phys. Lett.* **1990**, *167*, 524–526. [[CrossRef](#)]
24. Zhang, S.; Guo, F.; Yan, W.; Dong, W.; Zhou, J.; Zhang, W.; Xin, F.; Jiang, M. Perspectives for the microbial production of ethyl acetate. *Appl. Microbiol. Biotechnol.* **2020**, *104*, 7239–7245. [[CrossRef](#)]
25. van Wettere, B.; Aghakhani, S.; Lauwaert, J.; Thybaut, J.W. Ethyl acetate synthesis by direct addition of acetic acid to ethylene on a silicotungstic acid catalyst: Experimental assessment of the kinetics. *Appl. Catal. A Gen.* **2022**, *646*, 118849. [[CrossRef](#)]
26. Anli, R.E.; Bayram, M. Traditional Aniseed-Flavored Spirit Drinks. *Food Rev. Int.* **2010**, *26*, 246–269. [[CrossRef](#)]
27. Haas, Y.; Stein, G.; Tenne, R. The Photochemistry of Solutions of Eu(III) and Eu(II). *Isr. J. Chem.* **1972**, *10*, 529–536. [[CrossRef](#)]
28. Davis, D.D.; Stevenson, K.L.; King, G.K. Photolysis of europium(II) perchlorate in aqueous acidic solution. *Inorg. Chem.* **1977**, *16*, 670–673. [[CrossRef](#)]
29. Shu, D.; Wu, J.; Gong, Y.; Li, S.; Hu, L.; Yang, Y.; He, C. BiOI-based photoactivated fuel cell using refractory organic compounds as substrates to generate electricity. *Catal. Today* **2014**, *224*, 13–20. [[CrossRef](#)]
30. Zhang, B.; Fan, W.; Yao, T.; Liao, S.; Li, A.; Li, D.; Liu, M.; Shi, J.; Liao, S.; Li, C. Design and Fabrication of a Dual-Photoelectrode Fuel Cell towards Cost-Effective Electricity Production from Biomass. *ChemSusChem* **2017**, *10*, 99–105. [[CrossRef](#)]
31. Li, J.; Li, J.; Chen, Q.; Bai, J.; Zhou, B. Converting hazardous organics into clean energy using a solar responsive dual photoelectrode photocatalytic fuel cell. *J. Hazard. Mater.* **2013**, *262*, 304–310. [[CrossRef](#)]
32. Bai, J.; Wang, R.; Li, Y.; Tang, Y.; Zeng, Q.; Xia, L.; Li, X.; Li, J.; Li, C.; Zhou, B. A solar light driven dual photoelectrode photocatalytic fuel cell (PFC) for simultaneous wastewater treatment and electricity generation. *J. Hazard. Mater.* **2016**, *311*, 51–62. [[CrossRef](#)]
33. He, Y.; Yuan, R.; Leung, M.K. Highly efficient AgBr/BiVO₄ photoanode for photocatalytic fuel cell. *Mater. Lett.* **2019**, *236*, 394–397. [[CrossRef](#)]
34. He, Y.; Zhang, C.; Hu, J.; Leung, M.K. NiFe-layered double hydroxide decorated BiVO₄ photoanode based bi-functional solar-light driven dual-photoelectrode photocatalytic fuel cell. *Appl. Energy* **2019**, *255*, 113770. [[CrossRef](#)]

Disclaimer/Publisher's Note: The statements, opinions and data contained in all publications are solely those of the individual author(s) and contributor(s) and not of MDPI and/or the editor(s). MDPI and/or the editor(s) disclaim responsibility for any injury to people or property resulting from any ideas, methods, instructions or products referred to in the content.